NREL
NATIONAL RENEWABLE ENERGY LABORATORY

Appending High-Resolution Elevation Data to GPS Speed Traces for Vehicle Energy Modeling and Simulation

E. Wood, E. Burton, A. Duran, and J. Gonder

NREL is a national laboratory of the U.S. Department of Energy
Office of Energy Efficiency & Renewable Energy
Operated by the Alliance for Sustainable Energy, LLC

This report is available at no cost from the National Renewable Energy Laboratory (NREL) at www.nrel.gov/publications.

Technical Report
NREL/TP-5400-61109
June 2014

Contract No. DE-AC36-08GO28308

NREL
NATIONAL RENEWABLE ENERGY LABORATORY

Appending High-Resolution Elevation Data to GPS Speed Traces for Vehicle Energy Modeling and Simulation

E. Wood, E. Burton, A. Duran, and J. Gonder

Prepared under Task No. VTP2.2300

NREL is a national laboratory of the U.S. Department of Energy
Office of Energy Efficiency & Renewable Energy
Operated by the Alliance for Sustainable Energy, LLC

This report is available at no cost from the National Renewable Energy Laboratory (NREL) at www.nrel.gov/publications.

National Renewable Energy Laboratory
15013 Denver West Parkway
Golden, CO 80401
303-275-3000 • www.nrel.gov

Technical Report
NREL/TP-5400-61109
June 2014

Contract No. DE-AC36-08GO28308

NOTICE

This report is available at no cost from the National Renewable Energy Laboratory (NREL) at www.nrel.gov/publications.

Available electronically at http://www.osti.gov/scitech

Available for a processing fee to U.S. Department of Energy and its contractors, in paper, from:

U.S. Department of Energy
Office of Scientific and Technical Information
P.O. Box 62
Oak Ridge, TN 37831-0062
phone: 865.576.8401
fax: 865.576.5728
email: mailto:reports@adonis.osti.gov

Available for sale to the public, in paper, from:

U.S. Department of Commerce
National Technical Information Service
5285 Port Royal Road
Springfield, VA 22161
phone: 800.553.6847
fax: 703.605.6900
email: orders@ntis.fedworld.gov
online ordering: http://www.ntis.gov/help/ordermethods.aspx

Cover Photos: (left to right) photo by Pat Corkery, NREL 16416, photo from SunEdison, NREL 17423, photo by Pat Corkery, NREL 16560, photo by Dennis Schroeder, NREL 17613, photo by Dean Armstrong, NREL 17436, photo by Pat Corkery, NREL 17721.

Printed on paper containing at least 50% wastepaper, including 10% post consumer waste.

Acknowledgments

This research has been jointly supported by the U.S. Department of Energy's Vehicle Technologies Office and by the U.S. Department of Transportation's Federal Highway Administration. The authors would specifically like to thank Lee Slezak and David Anderson of the U.S. Department of Energy and Elaine Murakami of the U.S. Department of Transportation for their guidance and support. A special thanks to Sean Lopp of the National Renewable Energy Laboratory for contributing his statistical insight to this effort.

List of Acronyms

ADAS	Advanced Driver Assistance Systems
DEM	digital elevation model
GPS	global positioning system
NREL	National Renewable Energy Laboratory
USGS	United States Geological Survey

Executive Summary

Accurate and reliable global positioning system (GPS)-based vehicle use data are highly valuable for many transportation, analysis, and automotive considerations. Model-based design, real-world fuel economy analysis, and the growing field of autonomous and connected technologies (including predictive powertrain control and self-driving cars) all have a vested interest in high-fidelity estimation of powertrain loads and vehicle usage profiles. Unfortunately, road grade can be a difficult property to extract from GPS data with consistency.

In this report, we present a methodology for appending high-resolution elevation data to GPS speed traces via a static digital elevation model. Anomalous data points in the digital elevation model are addressed during a filtration/smoothing routine, resulting in an elevation profile that can be used to calculate road grade. This process is evaluated against a large, commercially available height/slope dataset from the Navteq/Nokia/HERE Advanced Driver Assistance Systems product. Results will show good agreement with the Advanced Driver Assistance Systems data in the ability to estimate road grade between any two consecutive points in the contiguous United States.

Table of Contents

List of Figures

List of Tables

1 Introduction

Accurate and reliable global positioning system (GPS)-based vehicle use data are highly valuable for many transportation, analysis, and automotive considerations. Model-based design, real-world fuel economy analysis and the growing field of autonomous and connected vehicle technologies (including predictive powertrain control and self-driving cars) all have a vested interest in high-fidelity estimation of powertrain loads and vehicle usage profiles [1–17].

Unfortunately, road grade can be a difficult property to extract from GPS data with consistency. While most GPS datasets do not contain explicit measurements of road grade, elevation is often estimated and can be used to calculate differentials for road grade estimates. However, depending on the distance between points, differential elevation must be measured with extremely high accuracy to produce grade estimates within reasonable error bounds (e.g., to measure road grade between points 100 m apart to within an absolute difference of ±0.1%, differential elevation must be accurate to within 0.1 m). While the two-dimensional accuracy of modern GPS devices (latitude/longitude coordinates) of plus or minus a few meters is generally acceptable for most applications, a far higher level of accuracy is required for elevation measurements to produce stable road grade values.

Modern GPS devices make estimates of elevation using similar triangulation techniques to those underlying two-dimensional coordinate readings. However, the accuracy of GPS-estimated elevation can vary by up to twice as much as two-dimensional estimates due to insufficient positioning and availability of the satellite network [18]. Compounded by the absence of standardization with respect to GPS elevation measurement protocols, road grade calculation directly from GPS-measured elevation is fraught with complications. References [19–21] provide additional documentation on GPS measurement techniques and quantified error statistics.

Several real-time techniques for estimating road grade independent of GPS-measured elevation have been validated and documented in the literature, including the use of:

- Kalman filters integrated with powertrain models and signals from the controller area network bus to simultaneously estimate vehicle mass and road grade [22–24]
- Filtered differential GPS velocity signals used as vectors to directly calculate instantaneous road grade (potentially requiring multiple runs over a given segment for estimates to converge) [25–30]
- Lidar units to measure differential elevation and distance, which are filtered and used to calculate the grade of the approaching roadway [31].

Unfortunately, these techniques are not applicable when attempting to append road grade to an existing database of two-dimensional GPS coordinates. Such a situation requires a reliable third-party dataset be employed to append the additional parameter of road grade to a GPS dataset.

We present a methodology for appending high-resolution elevation data to GPS speed traces via a digital elevation model (DEM). The use of a DEM is advantageous in that it provides defined static elevation values that enable consistency to be maintained between different GPS datasets and allows for elevation/grade values to be appended to data where GPS-measured elevation is

unavailable. Anomalous data points in the DEM are addressed during a filtration/smoothing routine, resulting in an elevation profile that can be used to calculate road grade. This process is evaluated against a large, commercially available height/slope dataset from the Navteq/Nokia/ HERE Advanced Driver Assistance Systems (ADAS) product. Results show good agreement with the ADAS data in the ability to estimate grade at any arbitrary point in the contiguous United States, including on all freeway, arterial, collector, and local roads.

2 Methodology

The methodology for appending high-precision elevation data to GPS data is divided into two processes: 1) the two-dimensional GPS coordinates are used to query a DEM, and 2) the resultant elevations are filtered to remove anomalous data and smoothed to produce stable road grade estimates.

2.1 Elevation Lookup

The premier DEM of the contiguous United States is widely considered to be maintained by the U.S. Geological Survey (USGS) (see Figures 1 and 2 for visual representations of the USGS DEM nationwide and the state of Colorado, respectively). Available in multiple resolutions, the 1/3-arc-second scale is employed herein as it is the highest resolution version that provides defined static elevation values for the entire continguous United States at approxomately 10-meter intervals (resulting in over 100 billion data points). In addition to its extensive coverage, the accuracy of the USGS DEM has been validated against a series of survey-quality data elevation markers with a reported root mean square error of 2.44 meters [32]. For further documentation on the USGS DEM, see [33, 34].

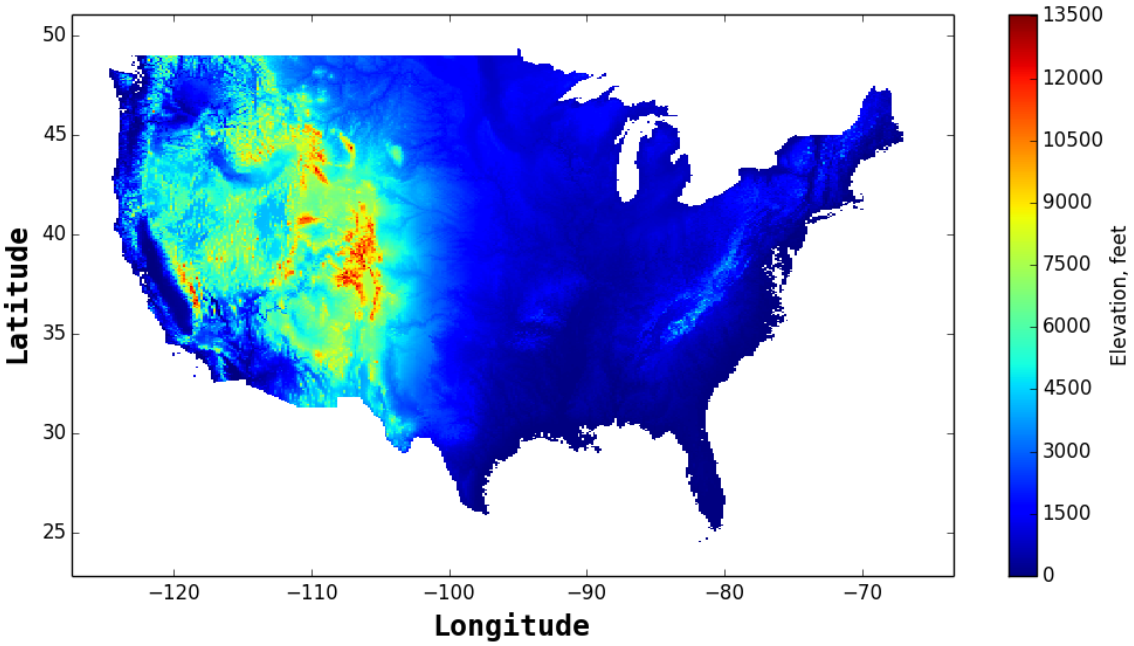

Figure 1. Elevation map of the contiguous United States produced using the USGS DEM

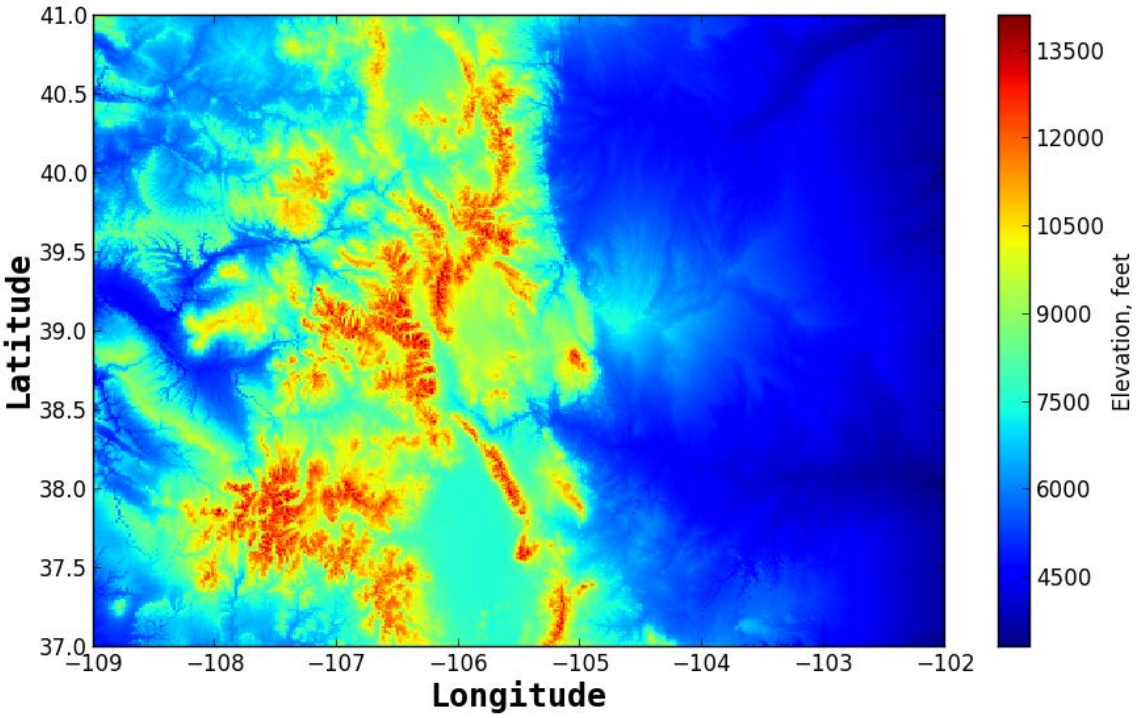

Figure 2. Elevation map of the state of Colorado produced using the USGS DEM

While the extent and accuracy of the USGS DEM make it an extremely powerful tool, consideration must be taken to house and query the database in an efficient manner. The USGS DEM is organized into a rectangular array of grid cells by geographic region with each directory containing multiple data files for sub-regions within the larger grid cell. When querying the DEM, the raw GPS coordinates are first converted into the World Geodetic System 84 geographic coordinate system [35] coincident with the DEM. Next, the point data are surveyed to identify the unique file locations for all grid cells traversed. Having identified the relevant file locations for an individual GPS trace, the data are reordered by grid cell to avoid multiple queries to an individual geographic region. Organizing the GPS data by grid cell maximizes computational resources by minimizing calls to the DEM. Elevation values for each grid cell are then extracted from the DEM in raster format, resorted according to the original GPS data, and appended to the database coincident with the appropriate source data.

It is important to note that the USGS DEM is a "bare-earth" dataset (as opposed to "top of canopy" DEMs) and as such, generally returns the lowest elevation at a given point. For instance, at river/bridge and highway/overpass intersections, the USGS DEM will return the lower of the two elevations (see Figure 3 for several examples of discontinuous intersections from downtown Denver, Colorado, where the USGS DEM is inlaid with maps and satellite imagery from Google). When matched to two-dimensional GPS coordinates from a vehicle speed trace, the USGS DEM returns sudden drops (and subsequent returns) in elevation of tens of feet. In the absence of additional processing, these sudden elevation changes would result in misrepresentative road grade values that would adversely affect subsequent calculations of drive cycle intensity and related fuel economy. In the next section, we discuss processing routines developed to identify such occurrences and filter elevation profiles accordingly.

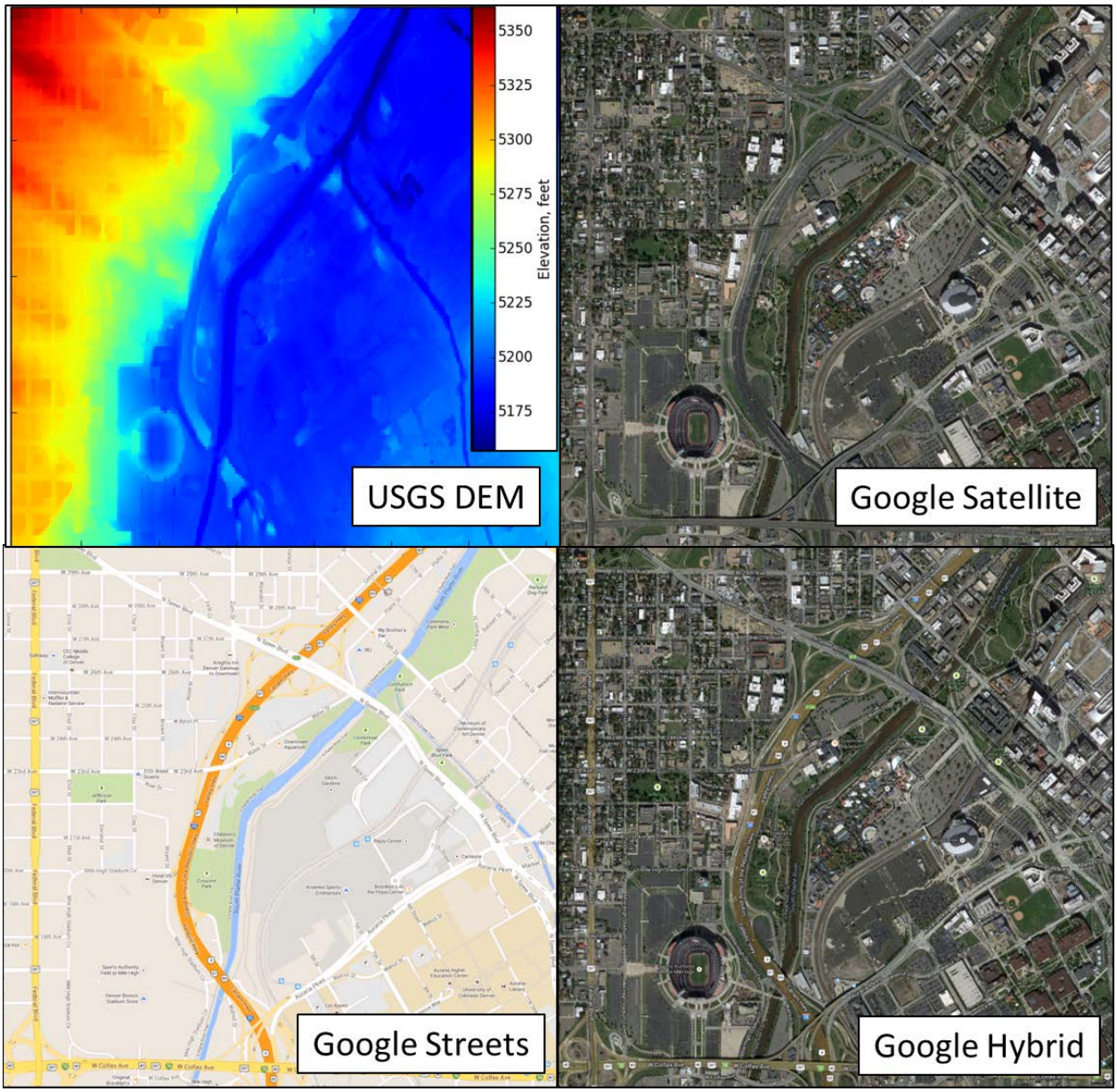

Figure 3. Coincident maps of downtown Denver, Colorado, produced using the USGS DEM, Google Maps Satellite layer, Google Maps Streets layer, and Google Maps Hybrid layer

(Google Maps credit: © 2014 Google, Map Data © 2014 Tele Atlas)

2.2 Data Filtration

After querying the DEM, raw elevations are adjusted using a multi-step filtration routine. This process seeks to remove errant elevation data associated with segments of elevated roadway (such as bridges and overpasses) and create smooth elevation profiles that result in continuous road grade signals for vehicle simulation. Parallels exist between these elevation filtration techniques and existing National Renewable Energy Laboratory algorithms for the filtration of

vehicle speed traces from GPS data [36]. The multi-step elevation filtration routine is outlined in five steps with corresponding images in Table 1.

Table 1. Step-by-Step Example of Elevation Filtration/Smoothing Performed on Sample Roadway

Step A: Raw elevation values versus distance.	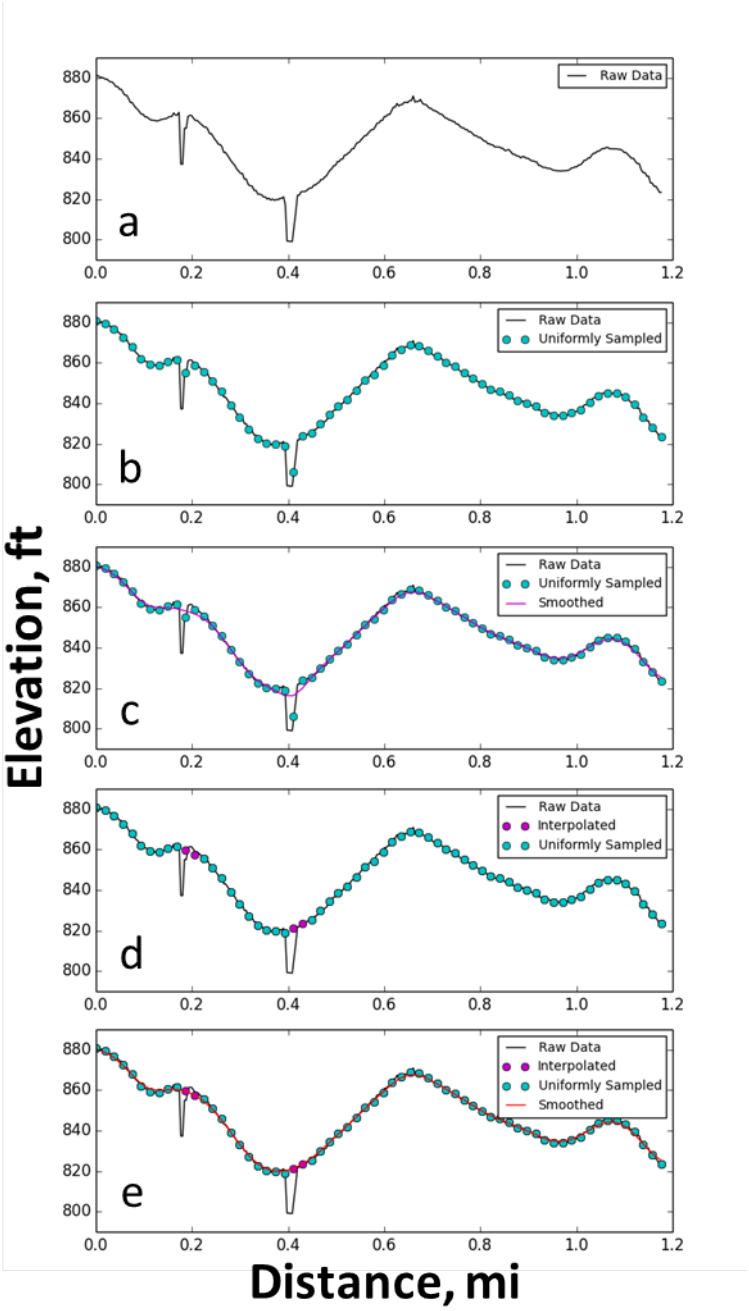
Step B: Elevation data are downsampled into uniformly spaced intervals, with each point representing the median value.	
Step C: Downsampled data are passed through a combined Savitzky-Golay and binomial filter (attenuating high frequncy noise), and the difference between pre-filtered and post-filtered elevation values are computed.	
Step D: Points where the elevation difference resulting from filtration exceeds a given value are discarded and backfilled via interpolation.	
Step E: The backfilled elevation profile is passed through the aforementioned combined Savitzky-Golay and binomial filter to eliminate noise from the distance derivative. Elevations at the orignal distance values are calculated via interpolation.	

After reviewing the elevation filtration process in great detail, we now highlight the net impact of the routine by examining the example raw versus filtered elevation and grade profiles in Figure 4. This plot highlights the two primary functions of the filtration routine: 1) the removal of errant data points, and 2) data smoothing. Errant data points are easily identified through

visual inspection of elevation profiles and are programatically identified via the filtration algorithm. Left unchanged, these dramatic drops in elevation would result in unrealistic grade values that are unsuitable for downstream vehicle simulation programs (instantaneous maximum power request from propulsion/braking system, inability of vehicle to maintain desired speed, potential for simulation results to be invalidated, etc.). While less visually apparent in the trace of raw elevation versus distance, the inherent noise for the duration of the raw road grade signal would result in unrealistic powertrain behavior were it attempted to be met as part of the drive cycle during powertrain simulation. Elevation smoothing removes such noise and provides stable grade signals.

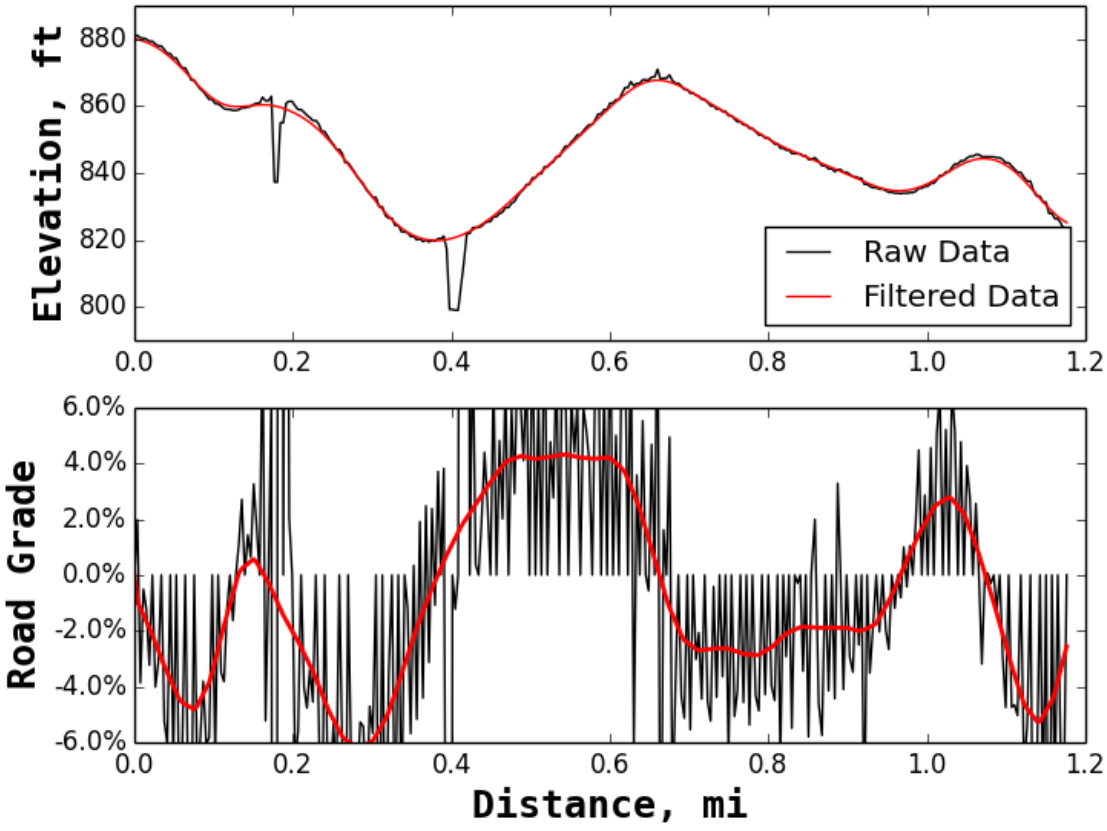

Figure 4. Raw versus filtered USGS elevation and road grade data

While the importance of elevation filtration has been highlighted in this section, particularly as it relates to vehicle powertrain simulation, we note that it generally does not have a transformational effect on the base layer USGS data. Over a representative sample of 53 million filtered elevation points from the National Renewable Energy Laboratory's Transportation Secure Data Center [37], 79% of the elevation values were adjusted by less than one foot and 96% of the elevation values were adjusted by less than five feet.

3 Validation

To evaluate the accuracy of this procedure for calculating road grade, we compare the results of our DEM-based road grade estimation with the Navteq/Nokia/HERE ADAS height/slope database of elevation and road grade values for approximately five million points in the contiguous United States [38]. The ADAS height/slope layer is a commercial data product containing road grade values for the majority of U.S. highways and select low capacity roadways. By validating our methods to roadways where the ADAS data have coverage, we expect to establish a reasonable level of confidence in our ability to estimate grade on all roadways.

For each point in the ADAS data, the corresponding links in the Navteq Streets layer are selected and used to populate a list of road-matched coordinates surrounding the selected point in both directions (if possible). These coordinates are then used to perform a lookup on the USGS DEM to append raw elevation values. These raw values are then filtered using the methods described in Section 2.2. Having both elevation and road grade data from the ADAS dataset and our filtered USGS DEM, the degree of agreement between these two data products can be evaluated. This evaluation will be presented in two sections with the first inspecting a short example section of roadway and the second contrasting the two datasets across large aggregations of data.

3.1 Example Roadway

First, we will examine an example section of roadway to compare filtered USGS values against ADAS data (see Figure 5). Inspection of the two elevation profiles and their associated derivatives reveals that while the general shapes of the filtered USGS and ADAS elevation profiles are similar, the filtered USGS elevation values exhibit a constant offset of approximately one hundred feet when compared to the ADAS dataset. The strong correlation in derived road grade coupled with the constant offset in elevation values suggests the disagreement in elevation can be attributed to the application of dissimilar global datums when determining absolute elevation [39–41]. Constant elevation offsets between readings from two different GPS devices are quite common, as each manufacturer will often use its own internal methodology for projecting elevation measurements from a global datum representing the sea level of the earth [42–43]. Such an offset, while significant in terms of absolute elevation, has no bearing on the calculation of road grade because it is defined as the derivative of the elevation with respect to distance traveled and is representative of the shape or profile of the data.

The lower graph in Figure 5 shows the absolute value of road grade as calculated from the filtered USGS elevation profile versus equivalent values from the ADAS dataset. While road grade is available as a signed value in both the USGS and ADAS datasets, comparisons between the two are made in terms of absolute values. The decision to perform the comparison on absolute values of road grade was made to limit user interpretation of direction of travel and its associated bias, and instead have the comparison focus on statistical trends in the underlying data. Given the large sample size of the dataset, any error introduced as a result of this decision is minimized due to the law of large numbers affixed to the central limit theorem. For the example road profile shown here, road grade values generally agree very well between the two datasets.

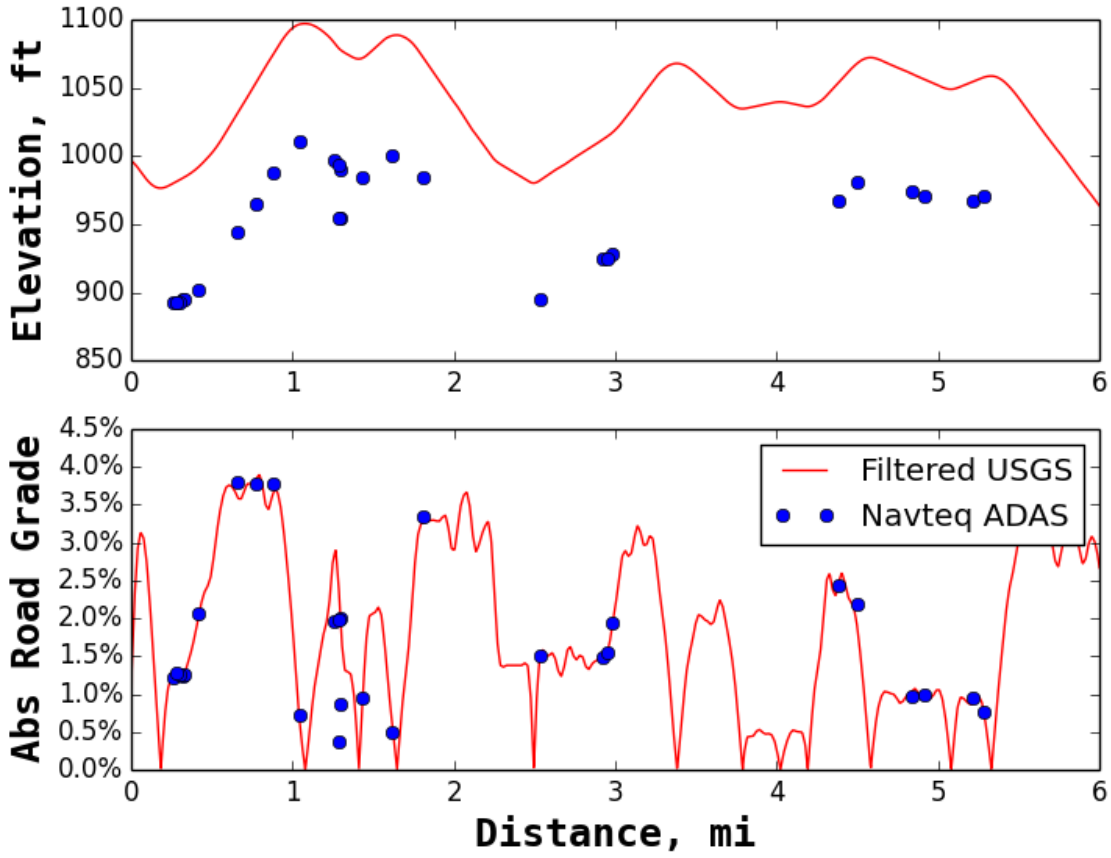

Figure 5. Sample elevation and road grade (absolute value) signals with filtered USGS data plotted as a red line and ADAS height/slope data overlaid as blue markers

3.2 Aggregate Comparisons

While example comparisons are useful in terms of disclosing comparison methods and results at the lowest level, larger aggregations of data are necessary to more broadly quantify the agreement between the USGS and ADAS datasets. To that end, the two data sets are segregated by road type and cumulative distributions of road grade are plotted for each (see Figure 6). Road type are classified using Navteq's definition of "functional class" where Functional Class 1 roads exhibit generally higher volumes and speeds and Functional Class 4 roads generally exhibit lower volumes and speeds. Table 2 presents more thorough definitions of the various functional classes.

Table 2. Navteq-Defined Road Functional Classes and Descriptions

Functional Class	Description
1	Roads with very few, if any speed changes, typically controlled access, and provide high volume, maximum speed movement between and through major metropolitan areas.
2	Roads with very few, if any speed changes, and provide high volume, high speed traffic movement. Typically used to channel traffic to (and from) Level 1 roads.
3	Roads which interconnect Level 2 roads and provide a high volume of traffic movement at a lower level of mobility than Level 2 roads.
4	Roads that provide for a high volume of traffic movement at moderate speeds between neighborhoods.
5	All other roads.

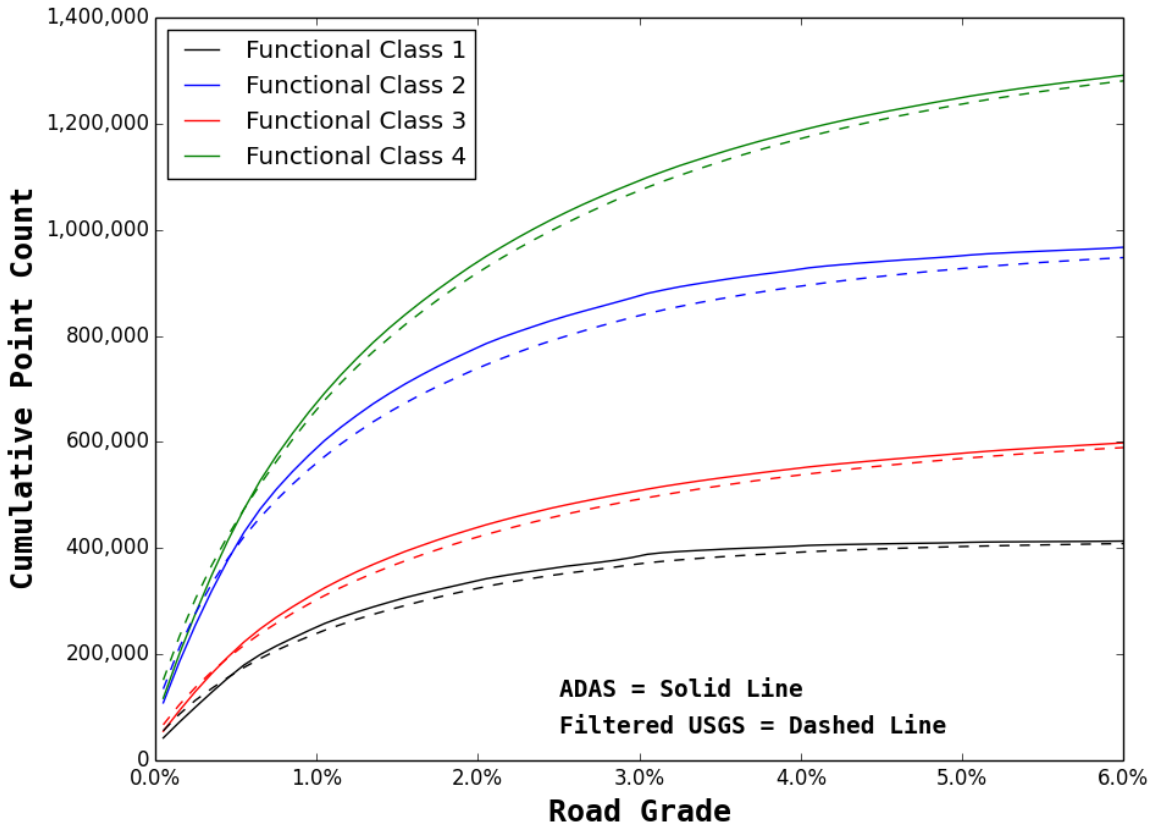

Figure 6. Cumulative distribution of road grade by functional class

A few observations from Figure 6 include:

- The ADAS dataset contains more points on Functional Class 2 and 4 roads than on classes 1 and 3. A count of roadways by functional class in the United States reveals that as the functional class increases, so does the number of roads (i.e., the majority of roads are low speed and capacity). Additionally, Navteq self-reports to have near 100% coverage of Functional Classes 1 and 2 in the ADAS dataset, while Functional Classes 3 and 4 are well below 50% coverage, and no data is available for Functional Class 5.
- The slope of the curves reveals that Functional Class 1 and 2 roads have a smaller share of data at steep road grades as compared to classes 3 and 4.
- The level of agreement between the filtered USGS and ADAS data is relatively strong, with the filtered USGS data generally exhibiting a slightly higher concentration of points at steep road grades. A chi-squared test reveals that the filtered USGS and ADAS distributions are samples of the same underlying distribution with a likelihood of >99.9%.

After examining the data by road type, the two datasets are next aggregated by geography. The cumulative distributions of road grade can be examined by state (see Figure 7). Five states, California, Colorado, Texas, Florida, and New York, are selected for their diverse distributions of road grade and relatively high volume of data.

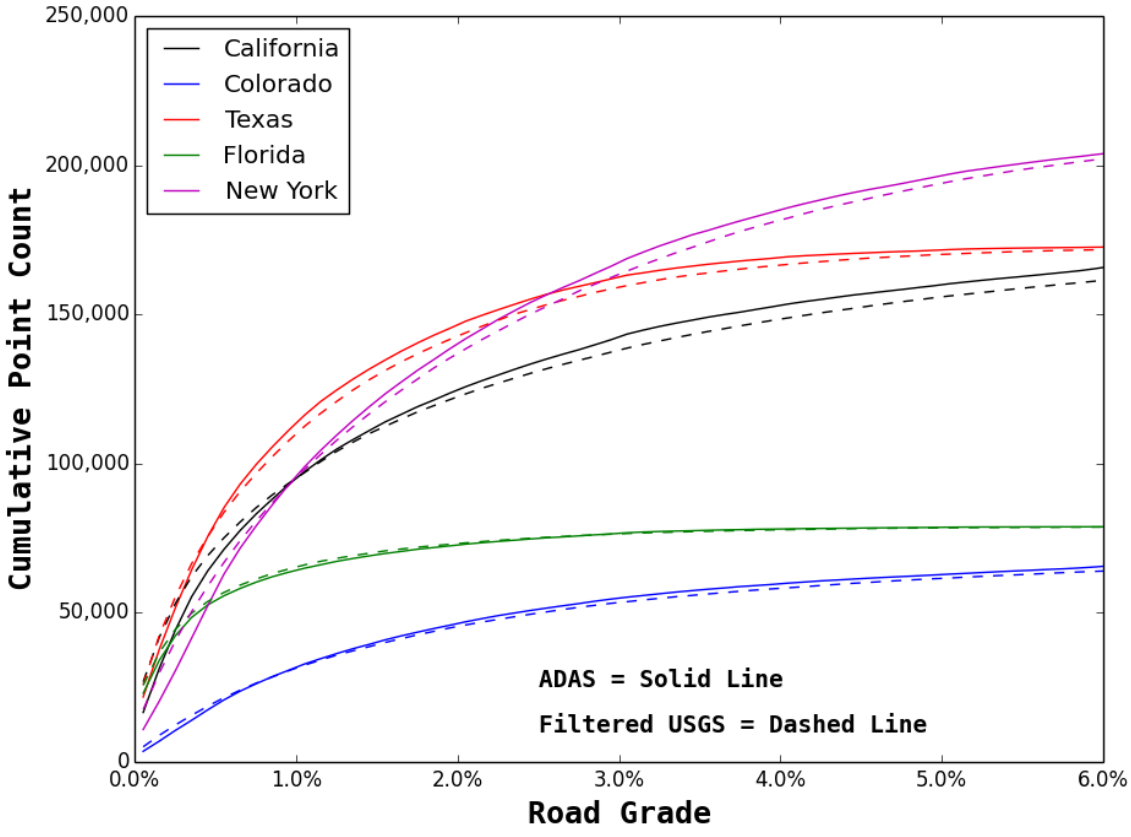

Figure 7. Cumulative distribution of road grade by geography

A few observations from Figure 7 include:

- The ADAS dataset contains more points for the states of California, Texas, and New York compared to Colorado and Florida (a trend mirrored by the size of the total road networks in each state).
- The slope of the cumulative distribution curves reveals that the states of California, Colorado, and New York tend to exhibit higher concentrations of steep road grade than the states of Texas and Florida.
- The level of agreement between the filtered USGS and ADAS data is relatively strong, with the filtered USGS data generally exhibiting a slightly higher concentration of points at steep road grades. A chi-squared test reveals that the filtered USGS and ADAS distributions are samples of the same underlying distribution with a likelihood of >99.9%.

While these cumulative distributions of road grade are encouraging in that the two datasets appear to contain similar trends with respect to road type and geography, a more rigorous comparison evaluating the distributions of road grade disagreement on a point-by-point basis is warranted. This comparison is presented in Figure 8, where distributions of road grade error by ADAS-reported road grade for Functional Class 1 roads are shown (similar distributions are observed in the data for Functional Classes 2 through 4 and therefore are omitted).

For the purpose of illustration, let us identify and describe two arbitrary points on this plot. Consider a marker existing in the ADAS grade bin of 0% with a filtered USGS error of +1.0%. Such a marker would have an ADAS-reported road grade with absolute value between 0% and 0.5% and a filtered USGS grade 1.0% steeper than the ADAS-reported value (overestimating road grade by 1.0%). Another example would be a point in the ADAS grade bin of 5% with a filtered USGS error of -2.0%. This point corresponds to data with an ADAS grade absolute value between 4.5% and 5.5% and a filtered USGS grade 2.0% less steep than the ADAS-reported value.

Having interpreted the layout of this plot, a few observations come to light:

- In terms of median value and interquartile range, the filtered USGS data tend to underestimate grade (more often than it overestimates) on grades steeper than 1% and tends to overestimate (more often than it underestimates) on grades less than 1% (all relative to ADAS data).
- The variance of each distribution tends to increase with grade.
- Extreme outliers are almost exclusively found in the overestimation region, a byproduct of the assumption that the filtered USGS data results in the correct sign for the estimated road grade (i.e., assuming the correct sign, it is impossible to underestimate a 3% grade by more than 3% grade).
- Outlier density stands out at low ADAS grades due to the overall high density of data at low grade values (i.e., the majority of points exist at low grade values).

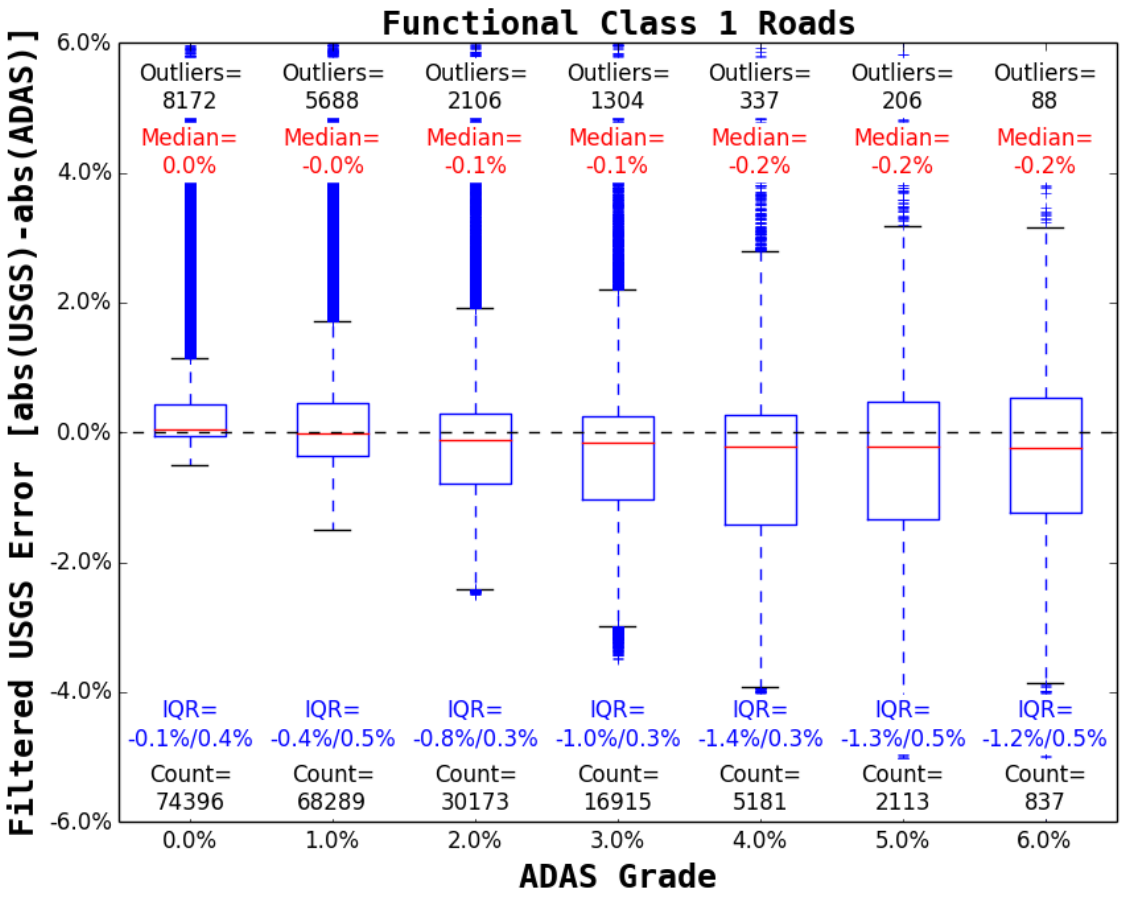

Figure 8. Distribution of road grade estimation error by ADAS road grade for Functional Class 1 roads

(Additional statistics included as text: point count, outlier point count, median, interquartile range)

It is worth noting that when taken in aggregate, median values for filtered USGS error are very nearly equal to zero for all functional classes of roadway.

While the agreement between the filtered USGS and ADAS datasets is quite good, there are certain instances of disagreement. Such instances are suspected to stem from one of the following sources:

- Erroneous measurements in the ADAS dataset
- Erroneous measurements in the USGS DEM
- Mistaken selection of two-dimensional coordinates leading up to ADAS points
- Limitations of filtration techniques (i.e., unintended filtration of good points or missed filtration of bad points).

In aggregate, over the millions of data points for which filtered USGS road grade was compared to the ADAS dataset, the aggregate root mean square error was 1.48% road grade.

4 Summary

A validated approach for appending high-precision elevation and road grade data to a series of GPS coordinates has been presented. A robust methodology for querying a static DEM and filtering/smoothing the resultant elevation profiles has been outlined. This methodology seeks to eliminate instances of sudden drops (and subsequent returns) in elevation and to dampen high frequency content in order to produce stable derivative signals of road grade. The agreement between the proposed method and a commercially available database of road grade has been quantified in several dimensions, including by road type, geography, and grade. Over millions of data points, the aggregate root mean square error of the presented method was found to be 1.48% road grade.

It has been demonstrated that road grade data can be extracted from the USGS DEM with a strong level of agreement to the commercially available ADAS height/slope data layer at the national level. While acknowledging the commercial value of the ADAS data, the USGS DEM provides the distinct advantages of being freely available as open data and having complete coverage over the contiguous United States and all roadways contained therein. This work is expected to be a valuable tool for researchers and engineers seeking to increase the fidelity of their work in the estimation of real-world fuel economy via modeling, simulation, and analysis.

References

1. Simpson, M.; Markel, T. "Plug-In Electric Vehicle Fast Charge Station Operational Analysis with Integrated Renewables." Preprint. International Battery, Hybrid, and Fuel Cell Electric Vehicle Symposium, May 2012. NREL/CP-5400-53914. Golden, CO: National Renewable Energy Laboratory, August 2012; 8 pp. Accessed April 21, 2014: http://www.nrel.gov/docs/fy12osti/53914.pdf

2. Attibele, P.; Makam, S.; Lee, Y.-L. "A Comparison of Real World and Accelerated Powertrain Endurance Cycles for Light-Duty Vehicles." Innovative Automotive Transmissions, Hybrid and Electric Drives, May 2013. Accessed April 21, 2014: http://www.nrel.gov/vehiclesandfuels/pdfs/chrysler_paper_posted_with_author_permission.pdf

3. Neubauer, J.; Wood, E. "Accounting for the Variation of Driver Aggression in the Simulation of Conventional and Advanced Vehicles." SAE World Congress, April 2013. NREL/CP-5400-58609. Golden, CO: National Renewable Energy Laboratory, August 8, 2013; 9 pp. Accessed April 21, 2014: http://www.nrel.gov/docs/fy13osti/58609.pdf

4. Lin, Z.; Dong, J.; Liu, C.; Greene, D. "Estimation of Energy Use by Plug-In Hybrid Electric Vehicles: Validating Gamma Distribution for Representing Random Daily Driving Distance." Transportation Research Board Annual Meeting, January 2012. Accessed April 21, 2014: http://pressamp.trb.org/conferenceinteractiveprogram/PresentationDetails.aspx?ID=48184&Email=

5. Khan, M.; Kockelman, K. "Predicting the Market Potential of Plug-In Electric Vehicles Using Multiday GPS Data." Transportation Research Board Annual Meeting, January 2012. (2012). Accessed April 21, 2014: http://www.caee.utexas.edu/prof/kockelman/public_html/TRB12PEVuse.pdf

6. Seaman, S.; Young, R. "Improving Survey Methods Using a New Objective Metric for Measuring Driving Time Variability in Survey and GPS Data." Transportation Research Board Annual Meeting, January 2012. (2012). Accessed April 21, 2014: http://trid.trb.org/view.aspx?id=1130665

7. Wood, E.; Neubauer, J.; Brooker, A.; Gonder, J.; Smith K. "Variability of Battery Wear in Light-Duty Plug-In Electric Vehicles Subject to Ambient Temperature, Vehicle Design, and Consumer Usage." Preprint. Electric Vehicle Symposium, May 2012. NREL/CP-5400-53953. Golden, CO: National Renewable Energy Laboratory, August 2012; 14 pp. Accessed April 21, 2014: http://www.nrel.gov/docs/fy12osti/53953.pdf

8. Smith, K.; Neubauer, J.; Earleywine, M.; Wood, E.; Pesaran, A. "Comparison of Plug-In Hybrid Electric Vehicle Battery Life across Geographies and Drive Cycles." SAE World Congress, April 2012. NREL/CP-5400-53817. Golden, CO: National Renewable Energy Laboratory, August 16, 2012; 11 pp. Accessed April 21, 2014: http://www.nrel.gov/docs/fy12osti/53817.pdf

9. Smith, K.; Earleywine, M.; Wood, E.; Pesaran, A. "Battery Wear from Disparate Duty Cycles: Opportunities for Electric-Drive Vehicle Battery Health Management." Preprint. American Control Conference, June 2012. NREL/CP-5400-54698. Golden, CO: National Renewable Energy Laboratory, October 2012; 9 pp. Accessed April 21, 2014: http://www.nrel.gov/docs/fy13osti/54698.pdf

10. Neubauer, J.; Brooker, A.; Wood. E. "Sensitivity of Battery Electric Vehicle Economics to Drive Patterns, Vehicle Range, and Charge Strategies," *Journal of Power Sources* (209), 2012; pp. 269–277. Accessed April 21, 2014: http://www.sciencedirect.com/science/article/pii/S0378775312005290

11. Neubauer, J.; Brooker, A.; Wood, E. "Sensitivity of Plug-In Hybrid Electric Vehicle Economics to Drive Patterns, Electric Range, Energy Management, and Charge Strategies." *Journal of Power Sources* (236), 2012; pp. 357–364. Accessed April 21, 2014: http://www.sciencedirect.com/science/article/pii/S0378775312011809

12. Gonder, J.; Earleywine, M.; Sparks, W. "Analyzing Vehicle Fuel Saving Opportunities through Intelligent Driver Feedback," *SAE International Journal of Passenger Cars – Electronic and Electrical Systems,* August 2012. NREL/CP-5400-53864. Golden, CO: National Renewable Energy Laboratory, April 16, 2012; 13 pp. Accessed April 21, 2014: http://www.nrel.gov/docs/fy12osti/53864.pdf

13. Earleywine, M.; Gonder, J.; Markel, T.; Thornton, M. "Simulated Fuel Economy and Performance of Advanced Hybrid Electric and Plug-In Hybrid Electric Vehicles Using In-Use Travel Profiles." IEEE Vehicle Power and Propulsion Conference, September 2010. NREL/CP-5400-48773. Golden, CO: National Renewable Energy Laboratory, 2010; 6 pp. Accessed April 21, 2014: http://www.nrel.gov/docs/fy13osti/48773.pdf

14. Gonder, J.; Markel, T.; Simpson, A.; Thornton, M. (2007). "Using GPS Travel Data to Assess Real World Driving Energy Use of Plug-In Hybrid Electric Vehicles (PHEVs)." *Journal of the Transportation Research Board – Sustainability, Energy, and Alternative Fuels*. Accessed April 21, 2014: http://www.nrel.gov/docs/fy07osti/40858.pdf

15. Tate, E.; Harpster, M.; Savagian, P. (2008). "The Electrification of the Automobile: From Conventional Hybrid, to Plug-In Hybrids, to Extended Range Electric Vehicles." SAE World Congress, April 2008. Accessed April 21, 2014: http://www.media.gm.com/content/dam/Media/microsites/product/volt/docs/paper.pdf

16. Neubauer, J.; Wood, E. (2014). "Thru-life Impacts of Driver Aggression, Climate, Cabin Thermal Management, and Battery Thermal Management on Battery Electric Vehicle Utility." *Journal of Power Sources* (259); pp. 262–275. Accessed April 21, 2014: http://www.sciencedirect.com/science/article/pii/S0378775314002766#

17. Neubauer, J.; Wood, E. "The Impact of Range Anxiety and Home, Workplace, and Public Charging Infrastructure on Simulated Battery Electric Vehicle Lifetime Utility." *Journal of Power Sources* (257), 2014; pp. 12–20. Accessed April 21, 2014: http://www.sciencedirect.com/science/article/pii/S0378775314000998

18. William J. Hughes Technical Center, NSTB/WAAS T&E Team. (2012). "Global Positioning System (GPS) Standard Positioning Service (SPS) Performance Analysis Report." Report #77. Submitted to Federal Aviation Administration GPS Product Team. Accessed April 21, 2014: http://www.nstb.tc.faa.gov/REPORTS/PAN77_0412.pdf

19. U.S. Department of Defense and GPS Navstar Global Positioning System. (2008). "Global Positioning System Standard Positioning Service Performance Standard." Accessed April 21, 2014: http://www.gps.gov/technical/ps/2008-SPS-performance-standard.pdf

20. U.S. Department of Transportation and Federal Aviation Administration. (2008). "Global Positioning System Wide Area Augmentation System (WAAS) Performance Standard." Accessed April 21, 2014: http://www.gps.gov/technical/ps/2008-WAAS-performance-standard.pdf

21. Clynch, J.R. "GPS Accuracy Levels." Department of Oceanography, Naval Postgraduate School. (2001). Accessed April 21, 2014: http://www.oc.nps.edu/oc2902w/gps/gpsacc.html

22. Winstead, V.; Kolmanovsky, I.V. "Estimation of Road Grade and Vehicle Mass via Model Predictive Control." *Proceedings of 2005 IEEE Conference on Control Applications*; 2005; pp. 1588–1593. Accessed April 21, 2014: http://ieeexplore.ieee.org/xpl/articleDetails.jsp?arnumber=1507359

23. McIntyre, M.L.; Ghotikar, T.J.; Vahidi, A.; Song, X.; Dawson, D.M. "A Two-Stage Lyapunov-Based Estimator for Estimation of Vehicle Mass and Road Grade." *IEEE Transactions on Vehicular Technology* (58:7), 2009; pp. 3177–3185. Accessed April 21, 2014: http://ieeexplore.ieee.org/xpls/abs_all.jsp?arnumber=4770202&tag=1

24. Kim, I.; Kim, H.; Bang, J.; Huh, K. "Development of Estimation Algorithms for Vehicle Mass and Road Grade." *International Journal of Automotive Technology* (14:6), 2013; pp. 889–895. Accessed April 21, 2014: http://link.springer.com/article/10.1007/s12239-013-0097-9

25. Bae, H.S.; Gerdes, J.C. "Command Modification using Input Shaping for Automated Highway Systems with Heavy Trucks." University of California Berkeley: California Partners for Advanced Transit and Highways (PATH), Research Report UCB-ITS-PRR-2004-48. 2004. Accessed April 21, 2014: http://www.escholarship.org/uc/item/1tv3z496

26. Sahlholm, P.; Jansson, H.; Kozica, E.; Johansson, K.H. "A Sensor and Data Fusion Algorithm for Road Grade Estimation." *Advances in Automotive Control* (5:1), 2007; pp. 55–62. Accessed April 21, 2014: http://www.diva-portal.org/smash/get/diva2:497247/FULLTEXT01.pdf

27. Ryan, J.; Bevly, D.; Lu, J. (2009). "Robust Sideslip Estimation using GPS Road Grade Sensing to Replace a Pitch Rate Sensor." *[Proceedings of] IEEE International Conference on Systems, Man and Cybernetics*, 2009; pp. 2026–2031. Accessed April 21, 2014: http://ieeexplore.ieee.org/xpls/abs_all.jsp?arnumber=5346320

28. Sahlholm, P.; Johansson, K.H. "Road Grade Estimation for Look-Ahead Vehicle Control using Multiple Measurement Runs." *Control Engineering Practice* (18:11), 2010; pp. 1328–1341. Accessed April 21, 2014: http://www.sciencedirect.com/science/article/pii/S0967066109001804

29. Sahlholm, P.; Johansson, K.H. "Segmented Road Grade Estimation for Fuel Efficient Heavy Duty Vehicles." [Proceedings] *2010 49th IEEE Conference on Decision and Control*; 2010; pp. 1045–1050. Accessed April 21, 2014: http://ieeexplore.ieee.org/xpls/abs_all.jsp?arnumber=5717298

30. Sahlholm, P.; Gattami, A.; Johansson, K.H. "Piecewise Linear Road Grade Estimation." SAE Technical Paper 2011-01-1039. 2011. Accessed April 21, 2014: http://kth.diva-portal.org/smash/get/diva2:503216/FULLTEXT01

31. Zhang, K.; Frey, H.C. "Road Grade Estimation for On-Road Vehicle Emissions Modeling using Light Detection and Ranging Data." *Proceedings, Annual Meeting of the Air & Waste Management Association, June 20-23, 2005, Minneapolis, MN*. 2005. Accessed April 21, 2014: http://www4.ncsu.edu/~frey/conf_pr/Zhang_Frey_2005.pdf

32. United States Geological Survey. "Vertical Accuracy of the National Elevation Dataset." *Digital Elevation Model Technologies and Applications: The DEM User's Manual, Second Edition*. Accessed April 21, 2014: http://ned.usgs.gov/documents/NED_Accuracy.pdf

33. United States Geological Survey. "The National Map." Accessed April 21, 2014: http://nationalmap.gov/viewer.html

34. United States Geological Survey. "National Elevation Dataset." Accessed April 21, 2014: http://ned.usgs.gov/

35. United Nations Office for Outer Space Affairs. "World Geodetic System 1984." Accessed May 27, 2014: http://www.oosa.unvienna.org/pdf/icg/2012/template/WGS_84.pdf

36. Duran, A.; Earleywine, M. (2012) "GPS Data Filtration Method for Drive Cycle Analysis Applications." SAE World Congress. April 2012. Accessed April 21, 2014: http://www.nrel.gov/docs/fy13osti/53865.pdf

37. National Renewable Energy Laboratory. "Transportation Secure Data Center." Accessed April 21, 2014: www.nrel.gov/tsdc

38. "Navteq Advanced Driver Assistance Systems." Accessed April 21, 2014: http://www.navteq.com/industries_automotive.htm

39. Trimble. “Trimble Survey Controller Software Online Help: Coordinate Systems, Geoids.” Accessed April 21, 2014: ftp://ftp.trimble.com/pub/tmsupport/Survey%20controller/CD/Trimble%20Survey%20Controller/Documentation/English/Help/Eng_SCCoordinate_Systems_AppendixA.htm#Geoid

40. Esri. “Coordinate Systems, Map Projections, and Geographic (Datum) Transformations.” Accessed April 21, 2014: http://resources.esri.com/help/9.3/arcgisengine/dotnet/89b720a5-7339-44b0-8b58-0f5bf2843393.htm

41. International Committee on Surveying and Mapping. (2012) “Fundamentals of Mapping.” Accessed April 21, 2014: http://www.icsm.gov.au/mapping/datums1.html#difference

42. Los Alamos National Laboratory. (2003) “GISLab: GPS Guide.” Accessed April 21, 2014: http://gislab.lanl.gov/gps_guide.html

43. Esri. (2003) “Mean Sea Level, GPS, and the Geoid.” Accessed April 21, 2014: http://www.esri.com/news/arcuser/0703/geoid1of3.html